AADE-20-FTCE-016

Foam Stability in Inclined Wells

Abhishek Govindu, Ramadan Ahmed, Subhash Shah, University of Oklahoma; Mahmood Amani, Texas A&M University at Qatar

Copyright 20209, AADE

This paper was prepared for presentation at the 2020 AADE Fluids Technical Conference and Exhibition held at the Marriott Marquis, Houston, Texas, April 14-15, 2020. This conference is sponsored by the American Association of Drilling Engineers. The information presented in this paper does not reflect any position, claim or endorsement made or implied by the American Association of Drilling Engineers, their officers or members. Questions concerning the content of this paper should be directed to the individual(s) listed as author(s) of this work.

Abstract

Foams can be generated to have a wide range of properties (density, viscosity, and stability). This unique behavior of foams makes them suitable for underbalanced drilling (UBD) in which downhole pressure is maintained below pore pressure. The stability of foam is critical to determine its hydraulics and cuttings transport capabilities. Foams that are stable and have good cleaning performance in vertical wells can lose their stability and subsequently their ability to transport solids in inclined wells. Thus, the main goal of this study is to investigate the effects of inclination, flow geometry, and shearing on the stability of aqueous foams. To achieve this, flow loop experiments were conducted to examine foam drainage at 72°F and 60 psi. The foam was generated in the flow loop and trapped in pipe and annular test sections to measure liquid drainage as a function of time. Two inclination angles were considered. For tests conducted in the annulus, the rotational speed of the inner rod was varied to examine the impact of shearing on foam drainage.

As expected, foam stability increased with quality. In the annulus, the wall effects hindered bubble and drained liquid motion, and consequently, delayed drainage. Hence, in the annulus, foam drained more slowly as compared to in the pipe. The formation of a liquid layer on the low-side of the inclined test sections (pipe and annulus) intensified drainage as the liquid flows downward freely and avoiding the hydraulic resistance of the foam structure. The effect of pipe rotation (shearing) on the foam drainage was minimal for the shear rate level considered in this investigation.

1. Introduction

Foams are simple colloidal systems with liquid as the continuous medium and gas as the dispersed phase. Gas dispersion creates a complex structure wherein bubbles are separated by thin layers of liquid (**Fig. 1**). Due to the packing of gas bubbles, foam exhibits greater viscosity than either of its constituent phases. The addition of gas to the system lowers its overall density and this density can be varied by controlling the volume of gas dispersed in liquid. Such properties make foam attractive as a drilling fluid, especially in underbalanced drilling (UBD) or when it is critical to minimize formation damage. Although foams are ubiquitous, they are not the natural stable state of liquid and gas phases. A gas and liquid system, at its most stable state, would exist with minimum surface contact between the two phases. To generate the complex bubble and liquid film structure of foam, energy must be added to the system, which is used to increase the surface area between the two phases, and hence, increases the surface energy of foam generated. The energy can be introduced into the system in the form of agitation, gas injection into liquid, or shearing a mixture of gas and the base liquid. The generation of foam can be aided by the presence of surface agents (surfactants) that lower the energy required.

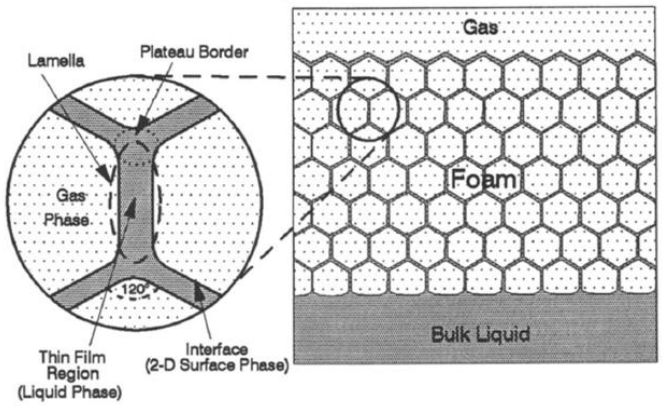


Fig. 1: Idealized foam structure (Schramm 1994)

1.1 Foam Drilling

Drilling foams are developed to take advantage of their low density to apply underbalanced drilling techniques and their high viscosity which is necessary for achieving good hole cleaning. In addition, they provide other benefits including large formation fluid handling capacity and reduced formation damage (Hutchison and Anderson 1972; Bentsen and Very 1976; Lincicome 1984; Anderson 1984). The application of drilling foam also minimizes differential sticking and increases rate of penetration (Paknejad et al. 2007). These unique properties have expanded the application of foam to low-pressure, depleted and highly fractured wells. Using conventional weighted drilling fluid in these types of wells, results in a high risk of lost circulation. In such cases, pre-formed foam fluids have shown greater success due to their low leak-off (Hall and Roberts 1984). Due to their low densities and compressibility, foam fluids have been used since the late 1980s

to drill reservoirs which are characterized by low pressures, extensive natural fractures, and high risk of formation damage. Foam is a viable alternative to air when drilling underbalanced, providing better solids carrying capacity and lower risk of wellbore instability (Nugroho et al. 2017). Replacing air with foam can also help prevent corrosion of tubulars and other downhole equipment by limiting their contact with oxygen (air encapsulated in bubbles) and formation water (Meng et al. 2005), and acting as a medium for corrosion inhibitors. There are economic benefits as well in using drilling foam. Due to low leak-off, less fluid is used overall, lowering costs. Furthermore, rig time is reduced, lowering operational expenditure because of the reduction in formation-damage, increased drilling rate, efficient hole cleaning, increased production rate, and increased oil recovery (Sui et al. 2000).

1.2 Foam Stability

Since foams are at a higher energy state, the process of phase separation or foam destabilization is spontaneous, i.e., does not require the addition of energy. Foams are, therefore, thermodynamically unstable, and they are destabilized from the moment of generation. The system tries to lose the excess surface energy and reduce the surface area between its liquid and gas phases. The most stable state is with liquid at bottom and gas on top, which occurs through two processes - foam drainage, where liquid flows downward from films between bubbles, and foam decay, which involves loss of bubble structure (Argillier et al. 1998). However, foams do not break instantaneously (unless prepared with pure liquids and gases). If a foam retains its bulk properties and does not undergo complete phase separation, while being utilized, it can be denoted as stable. In the case of drilling, for example, if foam fluid retains its properties for a duration exceeding circulation time, it can be called stable drilling foam. This can be quantified by using half-life, which is the time taken for the foam to lose half of its initial volume. The properties of foam, such as quality, bubble size, rheology, density, and overall stability, are interconnected and dependent upon the half-life of foam. Quality is usually used to term and denote foams. It is simply the gas volume fraction of foam.

The drainage process results in density variation along with foam structure. As liquid drains from the upper region of foam, it gets progressively wetter in the downward direction. Eventually, liquid separates from the foam structure and pools underneath it. This results in the thinning of liquid films between bubbles and pushes bubbles closer together, accelerating foam decay mechanism - smaller bubbles merge to form bigger ones as liquid films between them rupture (coalescence) and/or gas in smaller bubbles diffuse through very thin films into larger bubbles (coarsening). During coalescence in an open container, part of the gas phase escapes above a foam column (Cantat et al. 2013). There is no such loss of gas phase in bubble coarsening (Prud'homme and Khan 1997; Weaire and Hutzler 1999; Saint-Jalmes et al. 2005). Drainage and decay mechanisms acting on an aqueous foam (soap water and air) are shown in **Figs. 2** and **3**, respectively. The drainage behavior of various foams has been discussed in detail in an earlier study (Govindu et al. 2019). In this paper, the stability of aqueous foams is investigated with respect to the effects of inclination, conduit geometry, and external shear.

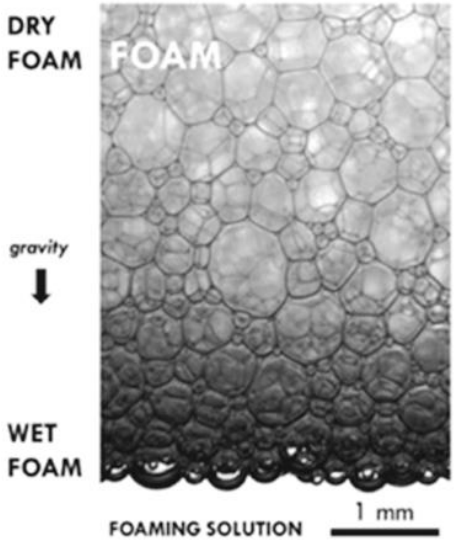


Fig. 2: Gravity drainage along foam structure (Drenckhan and Hutzler 2015)

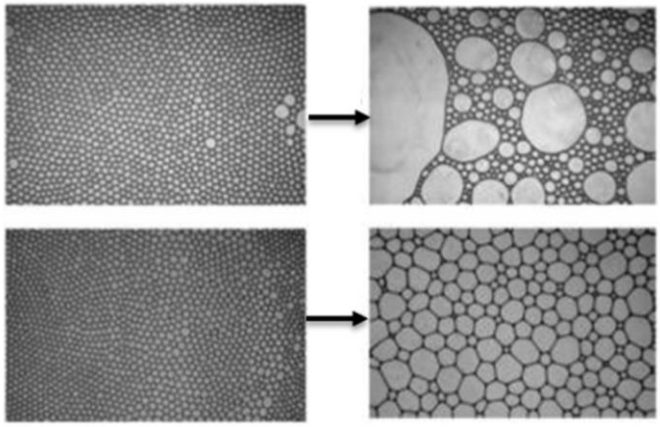


Fig. 3: Foam decay - coalescence (top) and coarsening (bottom) of bubbles (Hill and Eastoe 2017)

2. Literature Review

Although foam is thermodynamically unstable, free liquid and do not form instantly. Instead, the liquid must flow through the foam structure which is made of thin films. The film acts as a flow conduit for the drained liquid to flow and reach the bottom. The gas is trapped within these bubbles, unable to escape to the atmosphere above foam column without bubble coalescence. Gravity driven liquid movement is hindered by the viscosity of the liquid phase and capillary effects (Weaire and Hutzler 1999; Koehler et al. 2000). Viscous resistance experienced by the liquid within films increases as the quality of foam increases and films thin (Bhakta and Ruckenstein 1995; Monnereau et al. 1999). If the structure of foam does not change, i.e., bubble

network persists, eventually most of the liquid collects at the bottom and equilibrium state is achieved. At such an equilibrium state, foam structure contains residual liquid volume fraction which remains constant as the rate of drainage equals the rate of capillary suction at the free liquid-foam interface (Saint-Jalmes 2006). However, as liquid films thin, the rates of coalescence and bubble coarsening increase gradually, and at a critical liquid volume fraction, dependent upon gas and liquid properties, these rates are accelerated (Carrier and Colin 2003; Cantat et al. 2013). This is because diffusion through liquid films or film rupture is difficult when foam has high liquid content, and the decay mechanism is only dominant after it loses most of its liquid (Rio et al. 2014). Therefore, a high rate of drainage corresponds to an early onset of foam decay as well as a similar trend of the high decay rate. Effects of inclination, conduit geometry, and shear on foam drainage rate, hence, correspond to a similar effect on the decay rate. Foam undergoes multiple drainage equilibrium states and structural changes, before eventually completely collapsing.

The destabilization foam due to drainage and decay mechanisms varies with time. Hence, the drained liquid volume is presented against time to obtain a drainage curve. **Figure 4** shows the drainage curve of aqueous foam obtained under atmospheric conditions. Such curves have three characteristic regimes. The first regime corresponds to the moment after foam is generated where there is a lag time before the first drop of liquid exits the foam column followed by a rapid increase in drainage rate. During the second regime, the drainage rate is constant. During these two regimes, foam decay plays a little role and the structure of foam undergoes minor changes.

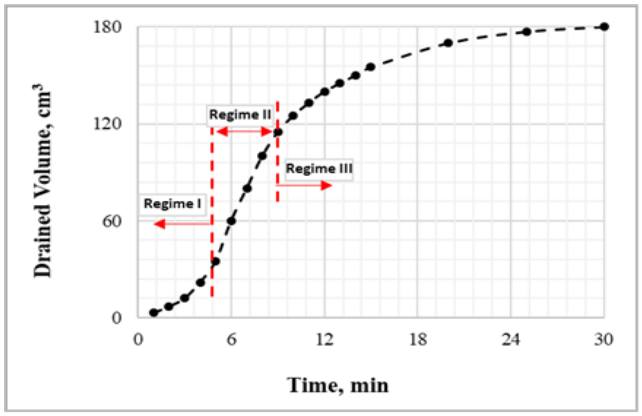


Fig. 4: Foam drainage curve (Govindu et al. 2019; Argillier et al. 1998)

In regime three, most of the liquid drains from the foam column, and hence, the drainage rate gradually decreases and tapers off into a plateau. At this stage, liquid drainage is greatly influenced by bubble coalescence and coarsening. Foam structure undergoes major changes during the third regime, and this lasts until the last bubble in foam column bursts resulting in complete separation of phases. The duration of each of these three regimes is dependent upon gas and liquid phases as well as surfactant type and concentration used to generate foam, the container in which the foam placed, the impurities present, ambient conditions (pressure and temperature), and other external factors (inclination, agitation)

2.1 Effect of Inclination

When vertical, the liquid volume fraction in a static foam column can be assumed to be constant laterally, varying significantly only in the axial direction. In inclined tubes and annuli, the liquid volume fraction varies both in axial and lateral directions (Stevenson 2007). Due to inclination, liquid follows the path of least resistance and drains towards the walls of the pipe or tube foam is captured in and accumulates. This accumulated liquid drains due to gravity along the walls and collects at the bottom (Dickinson et al. 2010). Further liquid draining from foam structure bypasses the complex film network and flows towards this flowing liquid film at the walls (**Fig. 5**). Since this flowing film does not experience viscous dissipation in thin films or resistance due to capillary forces, liquid drainage from foam column and free liquid accumulation at the bottom is accelerated (Mukhopadhyay et al. 2010). The angle of inclination of foam column has, therefore, considerable influence over foam drainage and its overall stability (Wang et al. 2013; Jiang et al. 2011). Wang et al. (2013) identified the critical angle, at which foam drainage rate was most enhanced at 45°.

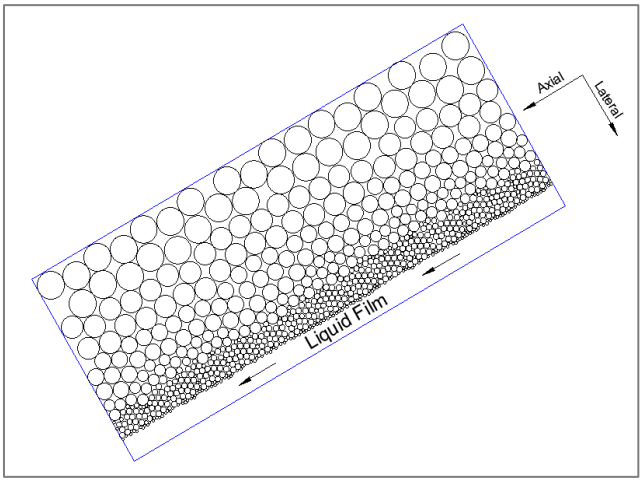


Fig. 5: Drainage of foam in inclined column (Govindu et al. 2019; Wang et al. 2013)

2.2 Effect of Container Walls

Most foam drainage studies are conducted in cylindrical tubes which are either made of glass or transparent plastics (Plexiglas) which enable visual observation. However, no comparative study was conducted until 2001 to investigate the influence of different diameters on liquid drainage. Forced drainage experiments of Brannigan and De Alcantara Bonfim (2001), where the liquid phase is injected at a fixed rate above the foam column, using vertical cylindrical tubes with 12.5, 18, 25, and 37.5 mm diameters showed that liquid drains faster in smaller diameter tubes. They theorized that liquid, in addition

to draining through the foam structure, also drains along with the thin liquid film that exists between foam and container walls. Such drainage experiences little resistance as liquid bypasses the complex bubble network where viscous resistance and capillary forces impede gravity-driven motion. This contribution to overall liquid drainage is significant for all diameters when containers are inclined as discussed in the previous section. However, when vertical, drainage along container walls is negligible compared to liquid draining from foam structure unless the diameter is very small. This is because interstitial films within foam structure significantly outnumber films along container walls. Drainage along wall films is significant if gas-liquid interfaces within foam are rigid (Koehler et al. 2004). In small-diameter containers, rigid or fixed gas-liquid interfaces are often observed. In large diameter containers, they tend to be more elastic.

2.3 Effect of Shear

There are limited studies investigating the effect of shear on the stability of foam. Under static conditions, liquid in foam structure possesses some yield stress which resists its movement or flow. If shear is applied to such a static foam column, this yield stress is overcome, enhancing gravity-induced liquid flow, and hence, resulting in rapid drainage (Goyon et al. 2010). This is a somewhat similar scenario to what happens when drilling with foam. A rotating drill string induces shear on foam in the annulus. However, shear exerted on the foam also adds energy to the fluid system, which might re-generate degraded foam.

3. Experimental Study

The stability of aqueous foams was investigated primarily by measuring the rate of liquid drainage in a static foam column. Parameters considered for these drainage studies were gas volume fraction, the inclination of the column, the geometry of container (pipe and annulus), and shear exerted on a foam column. In addition, the decay of foam structure was visually observed by capturing images and videos of trapped foam using a microscopic camera. Such images show gradual coarsening of foam structure and coalescence of bubbles, although it is not possible to differential these processes based solely on visual observation.

3.1 Scope of Study

Nine types of aqueous foams, differentiated based on gas volume fraction (foam quality), were considered for the foam drainage study. The upper and lower limit of foam quality was determined by the limitations of the experimental apparatus used to generate foam. The maximum quality of stable foam generated was 80% while the least quality was 40%. Between 40 and 80% quality, foam was homogenous. Out of this range, two-phase fluid was observed (slug flow of gas or liquid) when circulating in the flow loop. The nine foams considered were - 40, 45, 50, 55, 60, 65, 70, 75, and 80% quality. These foams were generated at a system pressure of, approximately, 689.48 KPa (100 psi) and captured in straight pipe and annulus of the same equivalent diameters. They were drained freely under ambient temperature conditions (22 ± 2 oC) at two different inclinations. The vertical scenario or 0o inclination served as the base line for the inclined case of 30o, measured from the vertical. Higher angles of inclination - 45 and 60o, were considered, but it was not possible to obtain consistent pressure measurements or drainage profiles. Foam trapped in vertical annulus was subjected to two shear rates, 1.5 and 1.8 s-1, by rotating the inner pipe. The air motor used to rotate the inner pipe was the limiting factor and the two shear rates correspond to its lower and upper limits. These experiments were limited to five foams - 40, 50, 60, 70, and 80% quality. Static drainage of foam in vertical annulus was used as the baseline to investigate the effect of shear on foam stability. All nine aqueous foams were used in the foam decay study, wherein these foams were trapped in a horizontal pipe section with a visual port.

3.2 Experimental Apparatus

The flow loop used to generate foams and study their drainage and decay (**Fig. 6**) consisted of -liquid reservoir, progressive cavity pump, nitrogen cylinder, foam generating section, pipe viscometers, stability testing cell, Coriolis flow meter, pressure gauges, temperature sensor, bleed and relief valves, and differential pressure transducer (Sherif et al. 2015a; 2015b; 2016a; 2016b). The base liquid phase was prepared in the liquid reservoir by adding the appropriate volume of freshwater and surfactant.

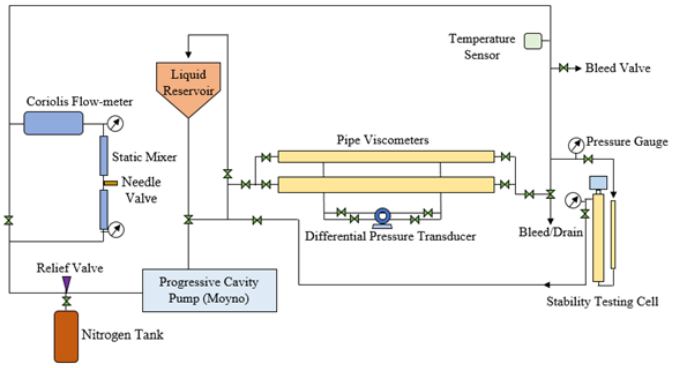


Fig. 6: Flow loop schematic (Govindu et al. 2019)

The progressive cavity pump (**Fig. 7**) had a variable speed controller and a maximum capacity of 113.56 L/min. The gas-phase was introduced into the flow loop using a nitrogen cylinder. The gas discharge was controlled using an absolute pressure gauge and valve. For personnel and equipment safety, a relief valve was installed and set to open if system pressure exceeded 1100 KPa. Foam generating section is comprised of a needle valve and static mixers (**Fig. 8**). The section can be bypassed using a valve to avoid foam generation. Consistent and homogeneous foam was generated and circulated through a pipe viscometer under laminar conditions. The differential pressure across the viscometer was measured and recorded to determine the rheological properties of the foams. Two

horizontal pipe viscometers (internal diameters of 24 and 32 mm) were used to measure the flow behavior of foam



Fig. 7: Progressive cavity pump

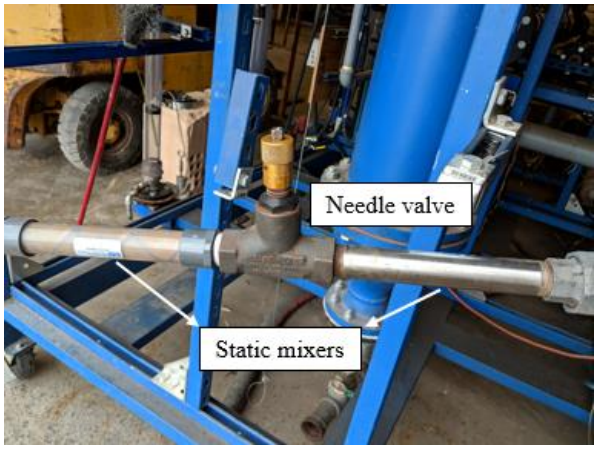


Fig. 8: Foam generation section

Foam stability testing section (**Fig. 9**) consisted of pipe and annular sections, a visual port, two pressure gauges, two absolute and eight differential pressure transducers, and a pneumatic regulator with air supply. The pipe and annular sections were mounted on a pivot such that they could be tilted from 0 to 90o (measured from the vertical). Straight pipe (Fig. 12) was made of clear polyvinyl chloride, enabling visual observation of fluid/foam contained in it. It had an inner diameter of 25 mm and a length of 1.08 m. A measuring tape was carefully attached to it to record the change in the level of liquid drained from foam.

The annular section had a polytetrafluoroethylene (PTFE) inner tubing and a stainless steel outer casing. The outer diameter of the PTFE tube was 50 mm and the inner diameter of the outer casing was 75 mm, resulting in a hydraulic diameter of 25 mm. The total length of the annular section was 1.22 m. This section also consisted of eight differential pressure transducers located at an equidistance of 152.4 mm, with the bottom-most one situated 75 mm above the base.

Air supply was regulated and provided to the low side of all eight transducers. The air pressure on the low side was measured using an absolute pressure transducer connected to the supply from a pneumatic regulator. The other transducer was connected to the top of the annular section and measured the pressure within it. The stability testing cell also consisted of a horizontal visual port (**Fig. 10**) to observe the decay of the foam structure trapped within it. A thin wire of 160 microns was attached to this port and used as a reference scale to estimate bubble diameters.

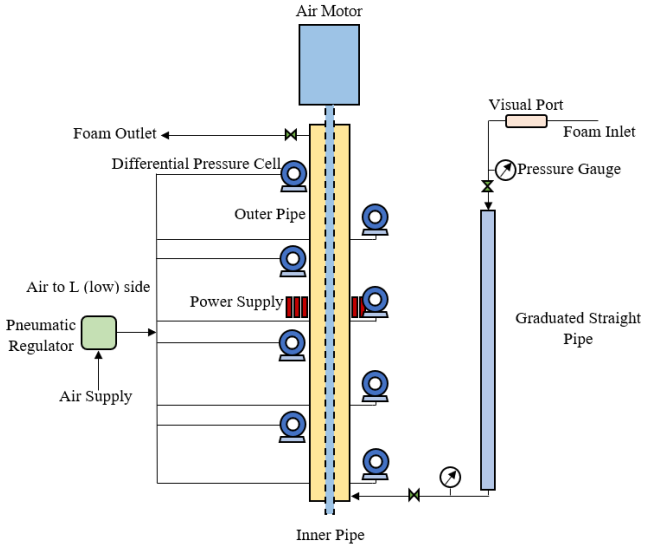


Fig. 9: Foam stability testing section (Govindu et al. 2019)

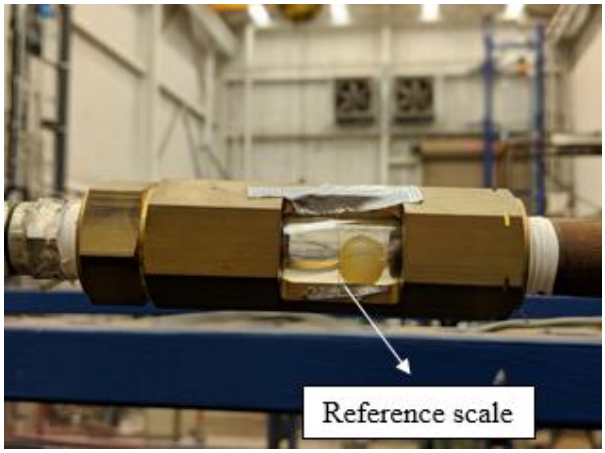


Fig. 10: Viewport with a reference scale

A data acquisition board was used to obtain signals from various sensors on the test loop and transmit to a computer in real-time. A program designed in VBA (Visual Basic Application) was used to transform these signals and display flow rate, density, temperature, and pressure, allowing constant monitoring. The flow rate of the pump and air supply to the eight differential pressure transducers could also be altered by sending signals to the variable frequency drive and pneumatic regulator, respectively, using this application. Air was supplied

in such a manner that the top-most differential pressure cell read a value of zero. Therefore, pressure measurements recorded by other transducers were the hydrostatic pressure exerted by fluid in the annulus. This system was calibrated each time before running an experiment to confirm signals transmitted to and from sensors on the flow loop were accurate, and that reliable data was recorded and displayed in appropriate units.

3.3 Materials Used

All foams were prepared with nitrogen as gas phase and water with 2% (v/v) anionic surfactant (AQF-2). Nitrogen was selected as it is used to prepare drilling foams due to its inert nature and non-flammability. Foam quality was evaluated using density measurements obtained from a Coriolis mass flow meter (Eq. 1), assuming the mass of the gas phase to be negligible. The foam quality was also back-calculated after the complete breaking of foam using the drained liquid volume (Eq. 2).

$$\Gamma = 1 - \frac{\rho_f}{\rho_L} \quad (1)$$

where ρ_f and ρ_L the densities of foam and base liquid, respectively.

$$\Gamma = 1 - \frac{V_L}{V_f} \quad (2)$$

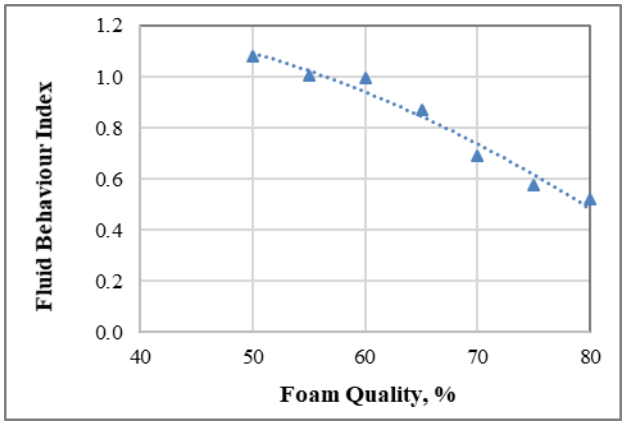
where V_f and V_L the volumes of base liquid and foam, respectively.

The quality obtained from Eq. 2 was slightly higher than the one measured using the flowmeter data. This inconsistency may be caused by slight changes in pressure along the flow path as foam travels from the foam generating section to the stability testing cell/section, resulting in the expansion of gas, increasing quality slightly.

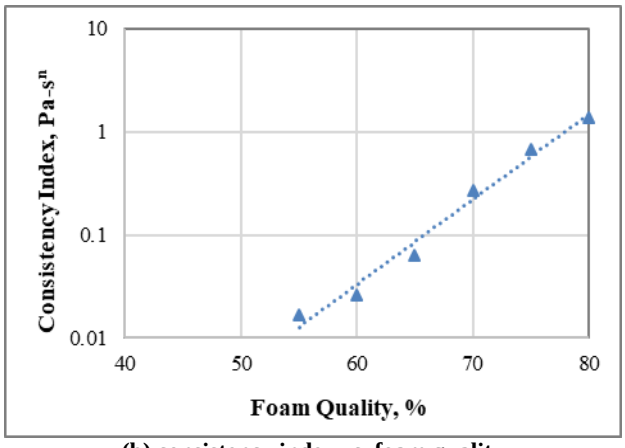
Consistent with previous studies (Chen et al. Sinha et al. 2019; Akhtar et al. 2018), foams exhibited non-Newtonian behavior and the power-law rheology model adequately characterized them. The power-law parameters (fluid behavior index and fluid consistency index of these fluids were calculated and are shown in **Fig. 11**. For low-quality foams (40 and 45%) it was not possible to estimate these parameters as the differential pressure measurements obtained from the two pipe viscometers were too low to be reliable. Values of n for 50 and 55% quality foams were slightly greater than 1. This could be due to the expansion of gas in foam as it flowed through the pipe viscometers, resulting in the recording of slightly higher differential pressures, leading to overestimation of wall shear stress corresponding to a fixed wall shear rate.

3.4 Procedure

In the present study, experiments were conducted to measure drained liquid volume as a function of time. Two approaches were used to obtain drained liquid volume: visually measuring liquid level (pipe) and monitoring liquid level using pressure sensors (annulus) as a function of time. The first step, before beginning experimental, was to calibrate the measurement system. The annular section was tilted to the angle of inclination under investigation and opened to the atmosphere. The air supply was shut-off and the readings of differential pressure transducers ensured to be zero. The annular section was then re-integrated into the flow loop and the air supply restored. The liquid phase was prepared in the reservoir by adding fresh water and an appropriate amount of anionic surfactant. The mixture was re-circulated at a low flow rate (19 L/min) to ensure homogeneity. The bleed valve was opened during this re-circulation, to ensure the system was purged of all gases. After purging, the flow was stopped, and the liquid was trapped in the annular section. The VBA application was then tested using the trapped liquid to calculate density profile across the annular section from hydrostatic pressure exerted by water over a height of 152.4 mm, recorded by the seven differential pressure transducers while the top-most one read zero. When properly calibrated, seven density readings were obtained corresponding to seven segments between the eight differential pressure transducers (**Fig. 12**). These values should be the same as water density (~ 1 g/ml) as the system contains only base liquid phase and no gas.



(a) fluid behavior index vs. foam quality



(b) consistency index vs. foam quality

Fig. 11: Power-law parameters of foams (data from Govindu et al. 2019)

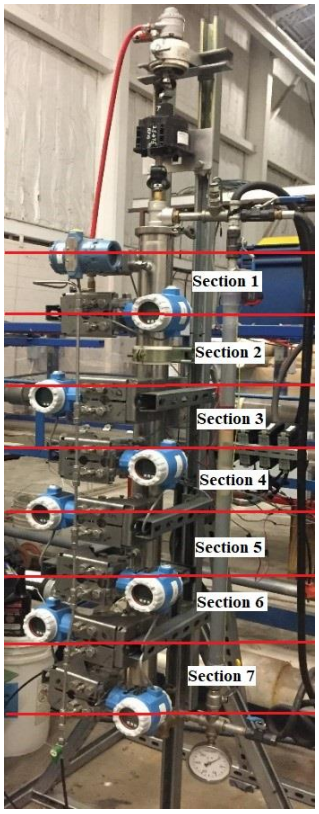


Fig. 12: Annular test section (Govindu et al. 2020)

During the test, foam was generated by removing the appropriate amount of liquid from the flow loop and introducing the gas phase (nitrogen) until the system pressure increased to 690 KPa (100 psi). Gas and liquid mixture was pumped at 37.85 L/min through the foam generating section. Here, the mixture was forced to follow a tortuous, spiral path of the static mixers, entraining gas in the liquid. Further energy required to create foam was provided by the needle valve which was manipulated such that the pressure difference across this valve was 206.84 KPa (30 psi). The gas-liquid mixture was circulated for 30 mins to ensure stable foam was created. This foam was then immediately captured in the pipe and annular sections, where it was allowed to drain freely without external influence. Liquid draining from foam in clear pipe was carefully measured using the measuring tape and time was recorded using a stopwatch. For this purpose, a flashlight was used to delineate the free liquid-foam interface at the bottom of the foam column. The VBA application recorded hydrostatic pressures in the seven segments of the annular section at fixed time intervals. These pressures were converted to density to create a density profile across the annulus. At the moment of foam capture in the annulus, hydrostatic pressures recorded varied linearly with depth as foam was homogeneous. With time, the liquid volume fraction varied spatially due to drainage and this relationship evolved into a non-linear one. Density profiles were generated form these hydrostatic pressures and averaged over a period of 50 s to reduce noise. **Figure 13** shows seven such profiles, each corresponding to a segment of the annulus, for 50% quality foam. In this figure, at the start, all segments read ~0.5 g/ml density of the stable and homogeneous foam. The experimental concluded when all seven profiles obtained from annulus plateaued, and liquid level measured from clear pipe remained unchanged with time.

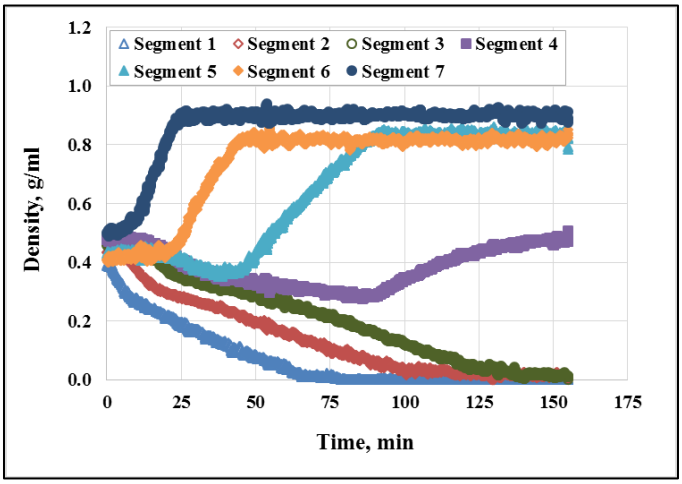


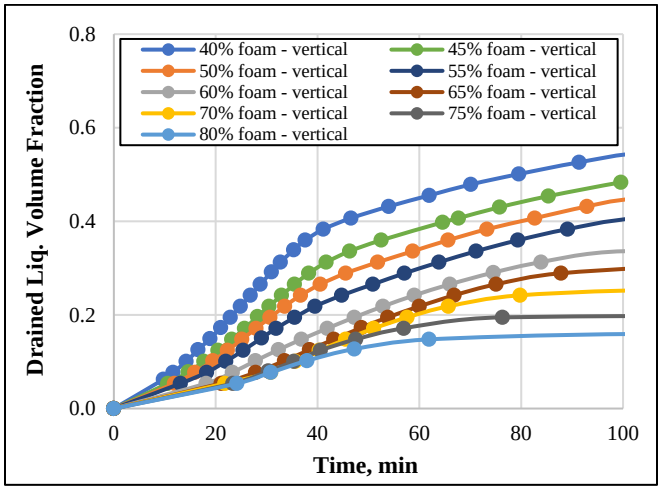
Fig. 13: Density profiles 50% quality foam in the annulus

Drainage curves were produced from experimental data gathered from pipe and annular sections. Cumulative drained liquid height data collected from clear pipe was plotted against the corresponding time to obtain a drainage curve. For the case of the annulus, the seven density profiles were used to generate data points, each corresponding to the appropriate time when the density of a segment approached that of liquid or gas phase. These curves were used to comparatively study the stability of the nine foams. Foam was also trapped in a horizontal section of pipe which had a visual port to observe changes in bubble structure over time. A microscopic camera was used to capture videos and images. Nine images were taken for each quality of foam under consideration starting with the first one taken when flow was stopped, and foam captured (t = 0). The rest were taken after geometrically progressive periods of 2, 4, 8, 16, 32, 64, 128, and 256 mins.

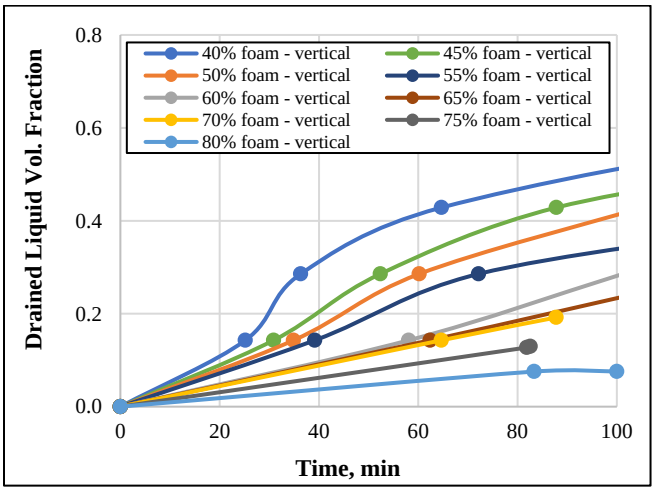
4. Results and Discussion

The drainage curves of foams obtained from vertically oriented pipe and annular sections are shown in **Fig. 14**. These curves are consistent with previously published measurements of liquid drainage from standing foams under atmospheric conditions (Argillier et al. 1998). The three distinct regimes discussed earlier can be seen in all drainage curves obtained – slow drainage rate followed by rapid increase, almost constant drainage rate, and a gradual decrease in liquid drainage culminating in a plateau until complete foam collapse. The drainage rate, characterized by the slope, of all curves shown in Fig. 14 decreased with increasing foam quality. This means the volume of liquid drained from high quality (dry) foam was lower as compared to low-quality foam (wet). Dry foams have complex bubble networks that are characterized by coarse

bubble sizes and thin liquid films. Draining liquid passes through a complex network of films where gravity drainage is opposed by viscous resistance and capillary forces. The effectiveness of these forces increases as the film thins (i.e., as foam quality increases). Conversely, these forces can be neglected in very wet foams which are characterized by thick films between small bubbles.



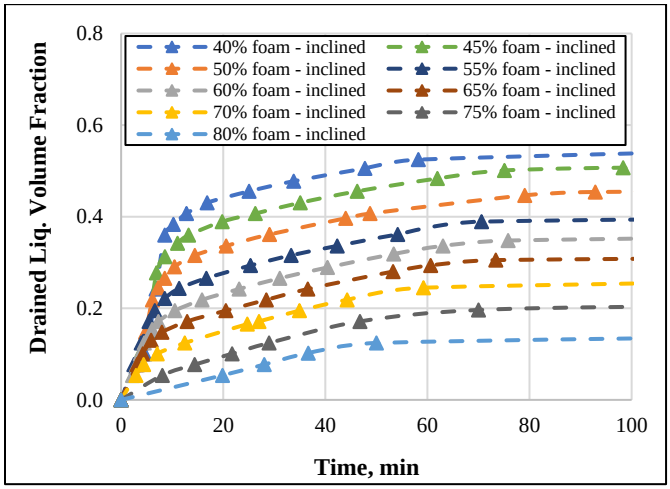
(a) pipe



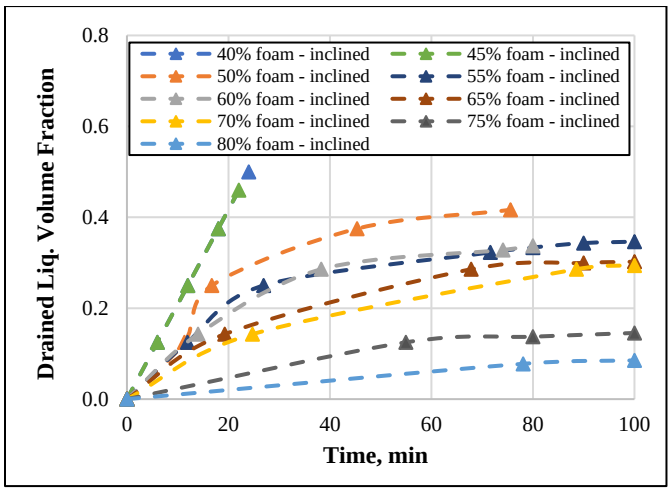
(b) annulus

Fig. 14: Drainage curves of foams in a vertical orientation (Govindu et al. 2019; 2020)

The drainage data obtained from the annular test section was limited as each data point corresponds to one of the seven segments being completely filled with drained liquid. At higher qualities, only the bottom segments were filled resulting in fewer data points as compared to low-quality foams. Comparing the data obtained from the pipe with the ones from the annulus, the drainage curves obtained from the pipe and the annulus are similar at low qualities (< 50%). At higher qualities (> 50%), more liquid was drained in the pipe as compared to the annulus for the same quality foam. In the annulus, the proximity of container walls would result in relatively more rigid gas-liquid interfaces which limits liquid flow over the casing as a wall-film, enhancing overall drainage (Brannigan and De Alcantara Bonfim 2001; Koehler et al. 2004). This is because drainage through interstitial films (foam structure) is hindered by viscous resistance and capillary forces while liquid draining as a wall-film is not. Furthermore, these forces are only effective in higher quality foams (> 50%) which are characterized by thin liquid films and are negligible in low-quality foams where films are very thick (< 50%).



(a) pipe



(b) annulus

Fig. 15: Drainage curves of foams in inclined orientation (Govindu et al. 2019; 2020)

Drainage curves obtained by inclining the test sections to 30° (measured from vertical) are shown in **Fig. 15**. The drainage behavior observed in inclined orientation is very similar to that observed in a vertical configuration. The drainage curves demonstrate the presence of the three regimes. The rate decreased with quality as observed in a vertical pipe and annulus. Also, it was lower in the annulus as compared to in the pipe for the same quality.

The drainage curves obtained from foams captured in a vertical annulus and subjected to a shear rate of 1.5 and 1.8 s^{-1} by rotating the inner pipe are shown in **Fig. 16**. It was hypothesized that the shear applied on a foam column would either break its structure, accelerating the drainage process, or supply energy to agitate the phases and regenerate foam, extending foam life. However, the air motor used to rotate the inner pipe was not able to generate enough shear to observe any measurable difference in the drainage curves of the five foams.

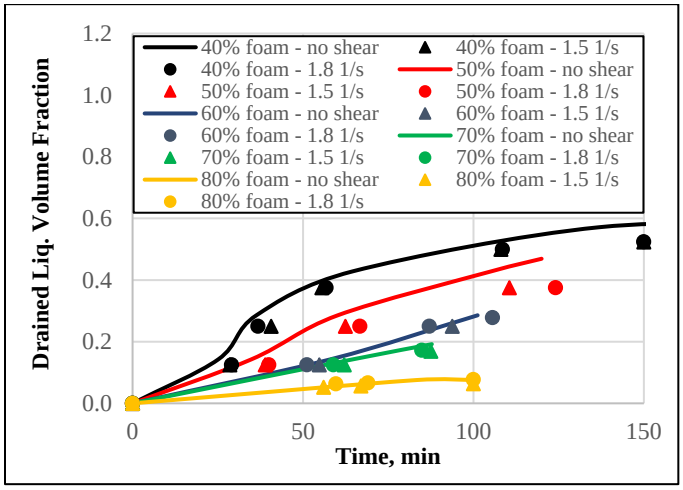


Fig. 16: Drainage curves of foam in an annulus with inner pipe rotation (Govindu et al. 2019; 2020)

Foam decay occurs through loss of bubble network by diffusion of smaller bubbles into larger ones (coarsening) and rupture of liquid film between bubbles (coalescence). The merging of bubbles in aqueous foams was observed and recorded with a microscopic camera. Images corresponding to 40% (wet) and 70% (dry) quality foams, taken at 2, 16, 64, and 128 mins after flow was stopped and foam was captured in a horizontal pipe that had a visual port (**Fig. 17)**.

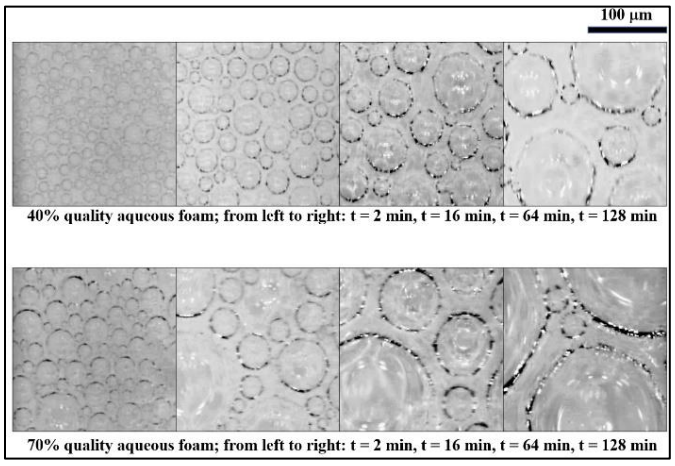


Fig. 17: Coarsening and coalescence of bubbles in 40 and 70% quality aqueous foams (Govindu et al. 2020)

Images were taken immediately after flow was stopped (within a period of 60 s), highlighting two bubbles into which smaller ones merged, are shown in **Fig. 18**. Higher quality foams contained larger bubbles on average. This is expected as higher quality foams have a larger volume fraction of gas-phase resulting in liquid distributed through very thin films separating relatively larger bubbles compared to wetter foams. The mean bubble size of foams increased with increasing time. This is due to liquid drainage, where the loss of liquid from films between bubbles results in the foam structure susceptible to foam decay processes of coarsening and coalescence (Rio et al. 2014; Carrier and Colin 2003).

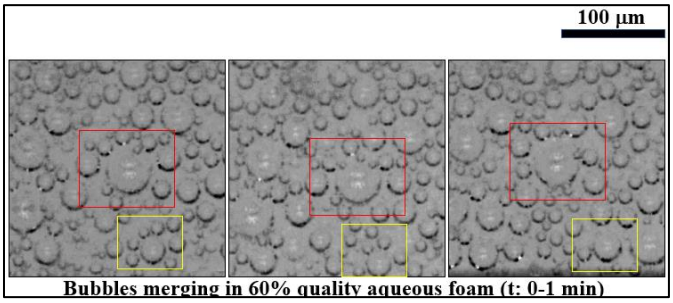


Fig. 18: Bubbles merging in 60% quality foam

5. Conclusions

The drainage behavior of aqueous foams was studied by trapping them in pipe and annulus. The drainage experiments were conducted in vertical and inclined configurations using pipe and annulus test sections. The following conclusions can be made based on these measurements and observations:

- Consistent with previous investigations conducted at atmospheric conditions, the drainage curves obtained showed three characteristic regimes.
- High-quality foams were more stable as they drained at a slower rate and had a prolonged life.
- Foams drained faster in pipe as compared to in annulus even though both conduits had approximately the same equivalent diameter.
- For a given quality foam, drainage is faster when the test section is inclined.
- The impact of shearing on the drainage behavior of foam is minimal for the shear rate range considered in this investigation.

Acknowledgments

This research was made possible by NPRP grant 10-0115-170165 from the Qatar National Research Fund. The authors would like to express gratitude to the Qatar National Research Fund (QNRF) and the University of Oklahoma.

References

1. Anderson, G.W. 1984. Use of Preformed Foam in Low Pressure Reservoir Wells. Proceedings, 5th Offshore SPE South East Asia Offshore Technology Conference, pp. 121–129.

2. Argillier, J. F., Saintpere, S., Herzhaft, B., Toure, A. 1998. Stability and Flowing Properties of Aqueous Foams for Underbalanced Drilling. SPE 48982, presented at the SPE Annual Technical Conference and Exhibition, New Orleans, Louisiana, September 27-30.
3. Akhtar, T.F., Ahmed, R., Elgaddafi, R., Shah, S. and Amani, M. 2018. Rheological behavior of aqueous foams at high pressure. Journal of Petroleum Science and Engineering, Vol. 162, 214-224.
4. Bentsen, N.W., Veny, J.N. 1976. Preformed Stable Foam Performance in Drilling and Evaluating Shallow Gas Wells in Alberta. Journal of Petroleum Technology, p. 1237–1240, August.
5. Bhakta, A., Ruckenstein, E. 1995. Drainage of Standing Foam. Langmuir, Vol. 11, p. 1486–1492.
6. Brannigan, G., De Alcantara Bonfim, O.F., 2001. Boundary effects on forced drainage through aqueous foam. Philosophical Magazine Letters 81, 197–201.
7. Cantat, I., Cohen-Addad, S., Elias, F., Graner, F., Höhler, R., Flatman, R., et al. 2013. Foams: structure and dynamics. OUP Oxford.
8. Chen, Z., Duan, M., Miska, S.Z., Yu, M., Ahmed, R.M. and Hallman, J. 2009. Hydraulic Predictions for Polymer-Thickened Foam Flow in Horizontal and Directional Wells, paper SPE 105583, Journal SPE Drilling & Completion, Volume 24, Number 1, Pages 40-49.
9. Carrier, V., Colin, A. 2003. Coalescence in draining foams. Langmuir, 19:4535 – 8.
10. Dickinson, J.E., Laskovski, D., Stevenson, P., Galvin, K.P. 2010. Enhanced foam drainage using parallel inclined channels in a single-stage foam fractionating column. Chemical Engineering Science, Vol. 65, p. 2481–2490.
11. Govindu, A, Ahmed, R., Shah, S., Amani, M. 2019. Stability of foams in pipe and annulus. Journal of Petroleum Science and Engineering, Volume 180, September, pages 594–604.
12. Govindu, A., Ahmed, R., Shah, S. Amani, M. 2020. Foam Stability - Does Well Inclination Matter? Paper SPE-199821-MS, accepted for presentation at the SPE/ICoTA Well Intervention Conference & Exhibition, 24-25 March, The Woodlands, Texas, USA.
13. Goyon, J., Bertrand, F., Pitois, O., Ovarlez, G. 2010. Shear Induced Drainage in Foamy Yield- Stress Fluids. Physical Review Letters, 104, 128301, 22 March.
14. Hall, D.L., Roberts, R.D. 1984. Offshore Drilling With Preformed Stable Foam. SPE-12794-MS, presented at SPE California Regional Meeting, Long Beach, California, 11-13 April.
15. Hill, C., Eastoe, J. 2017. Foams: From nature to industry. Advanced in Colloid and Interface Science, 247, p. 496–513.
16. Hutchison, S.O., Anderson, G.W. 1972. Preformed Stable Foam Aids Workover, Drilling. Oil and Gas Journal, September 25, p. 13–18.
17. Jiang, C.S., Wu, Z.L., Li, R., Liu, Q. 2011. Technology of protein separation from whey wastewater by two-stage foam separation. Biochemical Engineering Journal, Vol. 55, p. 43 – 48.
18. Koehler, S.A., Hilgenfeldt, S., Stone, H. 2004. Foam drainage on the microscale: II. Imaging flow through single plateau borders. Journal of Colloid and Interface Science, Vol. 276, p. 439 – 449.
19. Koehler, S.A., Hilgenfeldt, S., Stone, H.A. 2000. A Generalized View of Foam Drainage: Experiment and Theory. Langmuir 2000, 16, 6327-6341.
20. Lincicome, J.D. 1984. Using Foam to Drill Deep, Underpressured Zones. World Oil, p. 11–14, December 15.
21. Meng, Y., Wan, L., Yang, L., Wang, J. 2005. Discussion of Foam Corrosion Inhibition in Air Foam Drilling. SPE International Symposium on Oilfield Corrosion, SPE 94469.
22. Monnereau, C., Vignes-Adler, M., Kronberg, B. 1999. Influence of gravity on foams. Journal de Chimie Physique et de Physico-Chimie Biologique, 96:958 – 67.
23. Mukhopadhyay, G., Khanam, J., Nanda, A. 2010. Protein removal from whey waste water by foam fractionation in batch process. Separation Science and Technology, Vol. 45, p. 1331–1339.
24. Nugroho, W.A., Sumantri, M., Wibisono, D. 2017. Design and Application of Aerated and Foam Drilling Fluid, Case Study in Drilling Operations in Indonesia. SPE-186233-MS, presented at the SPE/IATMI Asia Pacific Oil & Gas Conference and Exhibition, Jakarta, Indonesia, 17-19 October.
25. Paknejad, A., Schubert, J.J., Amani, M. 2007. Foam Drilling Simulator. SPE-105338, presented at the 15th SPE Middle East Oil & Gas Show and Conference, Kingdom of Bahrain, 11-14 March.
26. Prud'homme, R.K., Khan, S.A. 1996. Foams: theory, measurements, and applications. Surfactant Science Series, Vol. 57.
27. Rio, E., Drenckhan, W., Salonen, A., Langevin, D. 2014. Unusually stable liquid foams. Advance Colloid Interface Science, Vol. 205, p. 74–86.
28. Saint-Jalmes, A. 2006. Physical chemistry in foam drainage and coarsening. The Royal Society of Chemistry, Soft Matter, 2, p. 836 – 849.
29. Saint-Jalmes, A., Durian, D., Weitz, D. 2005. Kirk-Othmer Encyclopedia of Chemical Technology. Fifth edition, Vol. 12, p. 1.
30. Schramm, L.L. 1994. Foams: Fundamentals and Applications in the Petroleum Industry. Advances in Chemistry Series 242, American Chemical Society, Washington DC.
31. Sherif, T., Ahmed, R., Shah, S. and Amani, M. 2015a. Rheological and Wall-Slip Behaviors of Polymer Based Drilling Foams. Paper 41552, presented at the Proceedings of the ASME 2015 34th International Conference on Ocean, Offshore and Arctic Engineering (OMAE2015), May 31-June 5, 2015, St. John's, Newfoundland, Canada.
32. Sherif, T., Ahmed, R., Shah, S. and Amani, M. 2015b. Rheological behavior of oil-based drilling foams, Journal

of Natural Gas Science and Engineering, Volume 26, September, Pages 873-882.
33. Sherif, T., Ahmed, R., Shah, S. and Amani, M. 2016a. Rheology of Oil-Based Drilling Foams. Paper 41552, Paper AADE-16-FTCE-81, presented at the AADE Fluids Technical Conference and Exhibition, April 12-April 14, Houston, Texas, USA.
34. Sherif, T., Ahmed, R., Shah, S. and Amani, M. 2016b. Rheological correlations for oil-based drilling foams, Journal of Natural Gas Science and Engineering, Volume 35, Part A, September, 1249-1260.
35. Sinha,V., Ahmed, R., Akhtar, T.F., Shah, S. and Amani, M. 2019. Rheology and hydraulics of polymer-based foams at elevated temperatures, Journal of Petroleum Science and Engineering, Volume 180, Pages 330-346.
36.
37. Stevenson, P. 2007. On the forced drainage of foam. Colloids and Surfaces A: Physiochemical Engineering Aspects, Vol. 305, p. 1 – 9.
38. Sui, Y., Cheng, X., Sun, Q., Ji, H. 2000. Research and Application of Recirculating Foam Drilling and Completion Fluid. IADC/SPE-59267, presented at the 2000 IADC/SPE Conference, New Orleans, Louisiana, 23-25 February.
39. Wang, Y., Wu, Z., Li, R., Zhang, Z. 2013. Enhancing foam drainage using inclined foam channels of different angles for recovering the protein from whey wastewater. Colloids and Surfaces A: Physicochemical and Engineering Aspects, Vol. 419, p. 28–36.
40. Weaire, D.L., Hutzler, S. 1999. The physics of foams. Oxford University Press.
41.